Department of Aerospace Engineering

Gas Turbine Propulsion laboratory (Proplab)

ANALYSIS OF THE EFFECTS OF METHANE INGESTION ON TURBOSHAFT ENGINES

Submitted To:

D.M.A. (Dave) Hollaway
Human Factors Engineering Manager
Offshore Risk and Integrity Services
ABSG Consulting, Inc.
15011 Katy Freeway, Suite 100
Houston, Texas 77094

Prepared By:

Paul G.A. Cizmas, Ph.D.
Gas Turbine Propulsion Laboratory (PropLab)
Texas A&M University
701 H.R. Bright Building
3141 TAMU
College Station, Texas 77843-3141

Contract No. TAMUS SRS 1504539

Date: 15 July 2015

ABSTRACT

This report presents an analytic investigation of the effect of methane ingestion on the power output of three turboshaft engines. These engines are representative for the power plants installed on helicopters used for offshore oil and gas logistical support on the U.S. Outer Continental Shelf (OCS). The results assess the change of the engine operating point due to methane ingestion and the likelihood of compressor stall and surge, or uncommanded power roll-back. This study examined a range of methane concentrations ranging from 1 to 18 percent by volume.

TABLE OF CONTENTS

ACRONYMS AND ABBREVIATIONS

APG – associated petroleum gas (methane, ethane, propane, butane)
API – American Petroleum Insitute
BSFC – brake specific fuel consumption
BSEE – Bureau of Safety and Environmental Enforcement
ECU – electronic control unit
EECU – electronic engine control unit
EEC – electronic engine controller
FADEC – full-authority digital engine control
FCU – fuel control unit
HMFC – hydromechancal fuel control
Jet A – aviation turbine fuel specification in accordance with ASTM D1655
LHV – lower heating value
N1 – gas producer turbine speed
N2 – power turbine speed
NTSB – National Transportation Safety Board
OCS – outer continental shelf
OPR – overall pressure ratio
PID – proportional-integral-derivative control
PLC – programmable logic controller
TAMU – Texas A&M University
TIT – turbine inlet temperature
TGT – turbine gas temperature
H – real static state at turboshaft inlet
H* – stagnation state at turboshaft inlet
1* – stagnation state at compressor inlet
2i* – ideal stagnation state at compressor exit
2* – stagnation state at compressor exit
3* – stagnation state at the exit from the combustor
4i* – ideal stagnation state at the exit from the gas generator turbine
4* – stagnation state at the exit from the gas generator turbine
45i* – ideal stagnation state at the exit from the power turbine
45* – stagnation state at the exit from the power turbine
5i – ideal static state at the exit nozzle
5 – real static state at the exit nozzle

LIST OF FIGURES

LIST OF TABLES

STATEMENT OF THE WORK

As a result of two helicopter mishaps and possibly others involving ingestion of associated petroleum gas (APG) during offshore logistical support of oil and gas exploration and production, the NTSB issued safety recommendations to the U.S. Department of the Interior, Bureau of Safety and Environmental Enforcement (BSEE), to address occurrences of total or partial loss of engine power on turbine-powered helicopters due to the ingestion of APG. As a result of these NTSB safety recommendations, BSEE issued a contract for aviation safety requiring the assessment of potential effects of methane or other combustible gases on helicopter operations.

To support this analysis, TAMU PropLab was contracted by ABS Group Aviation Safety Team to evaluate the effect of the ingestion of APG, specifically methane, on helicopter turboshaft engines. This analysis will:

- Determine the theoretical effect of methane ingestion on the power output of the representative turboshaft engines;
- Assess the change of the engine operating point due to methane ingestion;
- Assess the likelihood of compressor stall and surge, or uncommanded power roll-back due to methane ingestion; and
- Assess any difference in performance degradation resistance between the hydromechanical fuel control and Full Authority Digital Engine Control (FADEC).

METHODOLOGY

The analysis must determine the concentration of methane gas which may have a deleterious effect on the power output of various turboshaft engines. Since more than 90 percent of APG released from offshore installations is methane, only methane need be considered to produce a valid result.

It is not practical to look at each make, model, and turboshaft engine configuration used in helicopters. However, the bulk of helicopter turboshaft engines used on the OCS share common gas producer characteristics and fall into one of three categories:

- Joined multistage-axial and single-stage centrifugal compressor;
- Single-stage centrifugal compressor; or
- Split multistage-axial and single-stage centrifugal compressor.

Thus, the analysis may be completed by only analyzing the effects of methane ingestion on the three types of compressor configurations. Therefore, three representative turboshaft engines widely used in helicopter power applications are selected to perform this engineering analysis:

- Engine A has a single-stage centrifugal compressor section, a two-stage low-pressure gas generator turbine (N1), and two-stage high-pressure power turbine (N2) section
- Engine B has a joined multistage axial and single-stage centrifugal compressor section, a two-stage low-pressure gas generator turbine (N1), and two-stage high-pressure power turbine (N2) section;
- Engine C has a split single-stage axial and single-stage centrifugal compressor section, a single-stage gas generator turbine (N1), and a single-stage power turbine (N2) section.

These engines are chosen to represent a statistically valid sample of the helicopter turboshaft engine population operating on the OCS.

Due to the thermodynamic operating characteristics of gas turbine turboshaft engines, methane gas ingested into the engine could either be ignited through adiabatic compression heating above the autoignition temperature causing a compressor surge, or enrich the fuel causing an over-temperature condition with associated internal engine pressure increase, increase in compressor backpressure, or over-speed condition, all of which may cause a partial or total loss of engine power.

The engine response to methane ingestion was mathematically modelled using the required engine parameters to describe the real cycle power output at maximum takeoff power. These include the overall pressure ratio (OPR), mass airflow rate ($\dot{m}_{air}$) and power (hp). Additional parameters, including inlet diffuser efficiency, compressor efficiency, turbine inlet temperature (T_3), pressure drop in combustor section (Δp), combustor efficiency, mechanical losses, turbine efficiency, power turbine efficiency, differential pressure at nozzle expansion, and nozzle efficiency, are assumed to obtain a brake specific fuel consumption (BSFC) in µg/J at takeoff conditions when the pressure is one bar and the static temperature is 288.16°K. Engine operating parameters were derived from published engine operation and maintenance manuals, performance charts, and proprietary data provided by the engine OEM. Standard Jet A fuel is assumed in the real cycle computation such that the lower heating value (LHV) is 43,500 kJ-kg^{-1} (with the exception of Engine C which was 43,136 kJ-kg^{-1}) and the stoichiometric ration between mass flow rates and air and fuel was 14.66.

The real cycle for the three turboshaft engines was calculated using a numerical summation for enthalpy (kJ-kg^{-1}), temperature (°K), entropy (kJ-(kg-°K)$^{-1}$), and pressure (bar). These values are used to describe the theoretical effect of methane ingestion on the compressor (adiabatic compression ignition) and fuel enrichment on the combustor on the real cycle and thus power output of each representative engine. Fractions of methane ingestion are 0, 5, 10, and 15 percent by volume with all concentrations reported by mass.

The effect on the combustor and power output as a function of the turbine inlet temperature (TIT) as an expression of engine power output and was calculated from the energy conservation equation. The conservation of energy between the compressor and combustor is calculated as follows:

$$\dot{m}_{a1}h_a(T_2^*) + \dot{m}_{CH_4}\left(h_{CH_4}(T_2^*) + \xi_{CH_4}LHV_{Ch4}\right) + \dot{m}_f\left(h_f + \xi_{comb}LHV\right) = \dot{m}_{a_{left}}h_a(T_3^*) + \dot{m}_{\lambda=1}h_{\lambda=1} + \dot{m}_{proCH_4}h_{proCH_4}(T_3^*)$$

where:

- $\dot{m}_{a1}$ is the mass flow rate of air after methane injection;
- h_a is the enthalpy of air;
- $\dot{m}_{CH_4}$ is the mass flow rate of methane;
- ξ_{CH_4} is the efficiency of methane combustion;
- LHV_{Ch4} is the lower heating value (LHV) of methane;
- $\dot{m}_f$ is the mass flow rate of fuel (Jet A) prior to methane ingestion;
- h_f is the enthalpy of fuel;
- ξ_{comb} is the efficiency of Jet A combustion;
- *LHV* is the lower heating value of Jet A fuel;
- $\dot{m}_{a_{left}}$ is the mass flow rate of air that did not burn in the combustor;
- $\dot{m}_{\lambda=1}$ is the mass flow rate of combustion products resulting from the stoichiometric combustion of Jet A fuel;
- $h_{\lambda=1}$ is the enthalpy of combustion products resulting from the stoichiometric combustion of Jet A fuel;
- $\dot{m}_{proCH_4}$ is the mass flow rate of combustion products resulting from the stoichiometric combustion of methane;
- h_{proCH_4} is the enthalpy of combustion products resulted from the stoichiometric combustion of methane; and
- T_3^* is the turbine inlet temperature (TIT) in °K at stagnation.

Response to the changes in the turboshaft engine real cycle by various fuel control systems is qualitatively described.

ASSUMPTIONS AND LIMITATIONS

The methane ingestion in the compressor section is assumed to by uniform. Non-uniformity conditions are ignored but may cause local stall cells to form which are not predicted by this modelling.

Methane ingestion at the engine intake is assumed to be at the specified concentrations. The actual probability of these methane concentrations is dependent upon non-linear factors such as release rate, distance to source, wind magnitude and direction, and mechanical mixing of clean air into vapor cloud by the main rotor and are ignored.

Effects of local fluid strain rate and effect on autoignition and flame propagation is ignored. If fluid strain rate is considered, this would lower the probability of an autoignition.

Any ram pressure recovery at the compressor is ignored as this effect does not occur until 100 m/s forward airspeed (194 KTAS).

RESULTS

1. Turboshaft Engine Parameters

Three turboshaft engines were considered in this report: (1) ENGINE A has a single-stage centrifugal compressor, (2) ENGINE B has a six-stage axial and single-stage centrifugal compressor, and (3) ENGINE C has a single-stage axial and single-stage centrifugal compressor. This section presents the operating parameters the three turboshaft engines used in this analysis. The data was parametrically determined from published engine operation and maintenance manuals, performance charts, and proprietary data provided by the engine OEM.

1.1 Turboshaft Engine A

The engine operating parameters for Engine A are summarized in Table 1.

Table 1
Turboshaft Engine A

Parameter	Value
OPR	7.1
m_{air}	1.56 kg-s^{-1}
Power	370 hp

The following parameters shown in Table 2 were parametrically calculated and assumed to obtain a brake specific fuel consumption (BSFC) value of 120 μg/J at takeoff power conditions when the pressure was one bar and the static temperature was 288.16°K. Standard fuel (Jet A) was assumed in the real cycle computation such that the lower heating value (HLV) was 43,500 kJ-kg^{-1} and the stoichiometric ratio between mass flow rates of air and fuel was 14.66.

Table 2
Operational Parameters
Turboshaft Engine A

Parameter	Value
Inlet Diffuser Efficiency, η_{diff}	98%
Compressor Efficiency, η_c	82.5%
Turbine Inlet Temperature, T_3^*	1,436°K
Pressure Drop in Combustor, Δ_p	3%
Combustor Efficiency, ξ_{comb}	90%
Mechanical Losses	5%
Gas Producer Turbine Efficiency, η_t	89%
Power Turbine Efficiency, η_t	87%

From these parameters, compressor maps for efficiency, mass flow rate, and pressure ratio were constructed as shown in Figures 1 and 2.

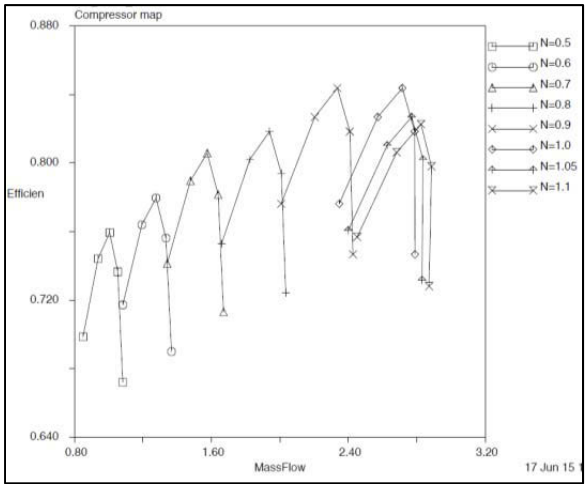

Figure 1: Compressor Efficiency Map for Engine A

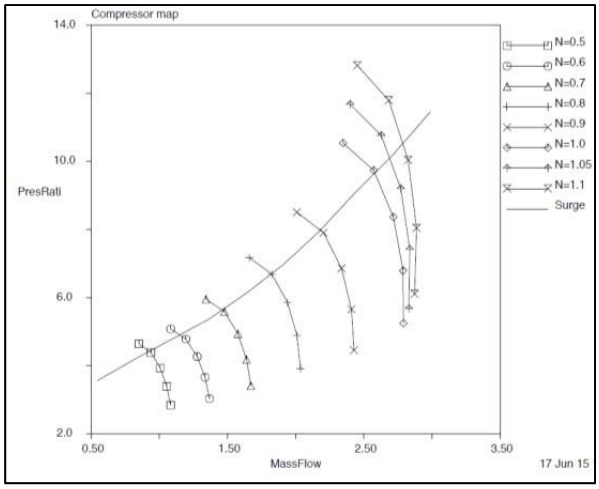

Figure 2: Mass Flow v. Pressure Ratio Map for Engine A

1.2 Turboshaft Engine B

The engine operating parameters for Engine B are summarized in Table 3.

Table 3
Turboshaft Engine B

Parameter	Value
OPR	9.2
$\dot{m}_{air}$	2.77 kg-s^{-1}
Power	600 hp

The following parameters shown in Table 4 were parametrically calculated and assumed to obtain a brake specific fuel consumption (BSFC) value of 108.4 μg/J at takeoff power conditions when the pressure was one bar and the static temperature was 288.16°K.

Standard fuel (Jet A) was assumed in the real cycle computation such that the lower heating value (HLV) was 43,500 kJ-kg^{-1} and the stoichiometric ratio between mass flow rates of air and fuel was 14.66.

Table 4
Operational Parameters
Turboshaft Engine B

	Value
Inlet Diffuser Efficiency, η_{diff}	98%
Compressor Efficiency, η_c	85%
Turbine Inlet Temperature, T_3^*	1,410°K
Pressure Drop in Combustor, Δ_p	6%
Combustor Efficiency, ξ_{comb}	100%
Mechanical Losses	5%
Gas Producer Turbine Efficiency, η_t	92%
Power Turbine Efficiency, η_t	89%

From these parameters, compressor maps for efficiency, mass flow rate, and pressure ratio were constructed as shown in Figures 3 and 4.

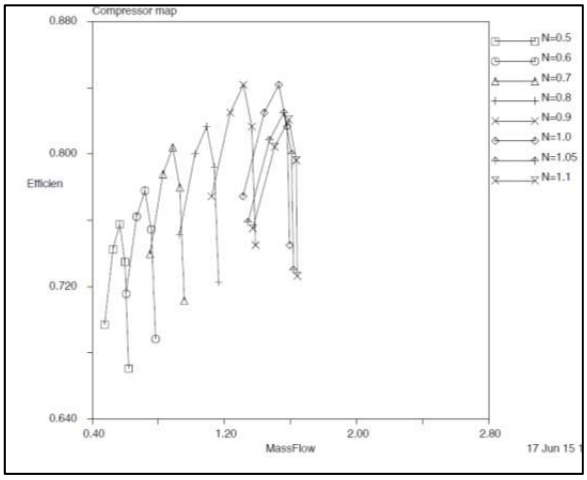

Figure 3: Compressor Efficiency Map for Engine B

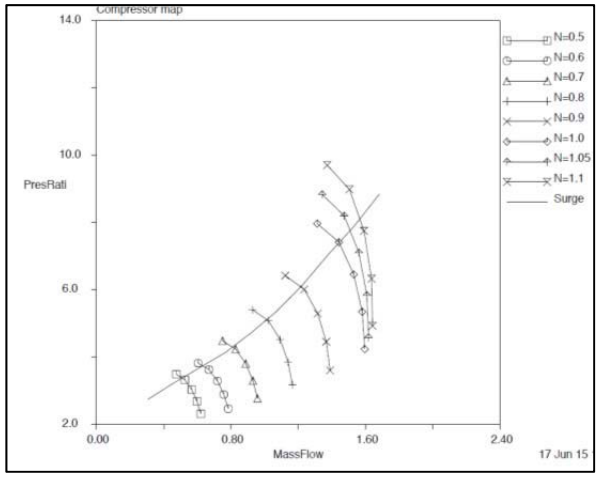

Figure 4: Mass Flow v. Pressure Ratio for Engine B

1.3 Turboshaft Engine C

The engine operating parameters for Engine C are summarized in Table 5.

Table 5
Turboshaft Engine C

Parameter	Value
OPR	8.0
$\dot{m}_{air}$	2.50 kg-s^{-1}
Power	779 hp

The following parameters shown in Table 6 were parametrically calculated and assumed to obtain a brake specific fuel consumption (BSFC) value of 82.9 μg/J at takeoff power conditions when the pressure was one bar and the static temperature was 288.16°K. Standard fuel (Jet A) was assumed in the real cycle computation such that the lower heating value (HLV) was 43,136 kJ-kg^{-1} and the stoichiometric ratio between mass flow rates of air and fuel was 14.66.

Table 6
Operational Parameters
Turboshaft Engine C

Parameter	Value
Inlet Diffuser Efficiency, η_{diff}	100%
Compressor Efficiency, η_c	80%
Turbine Inlet Temperature, T_3^*	1,400°K
Pressure Drop in Combustor, Δ_p	3.5%
Combustor Efficiency, ξ_{comb}	92%
Mechanical Losses	5%
Gas Producer Turbine Efficiency, η_t	93.7%
Power Turbine Efficiency, η_t	89%
Pressure Difference at Nozzle Expansion	8.6%
Nozzle Efficiency, η_{nozzle}	96%

From these parameters, compressor maps for efficiency, mass flow rate, and pressure ratio were constructed as shown in Figures 5 and 6.

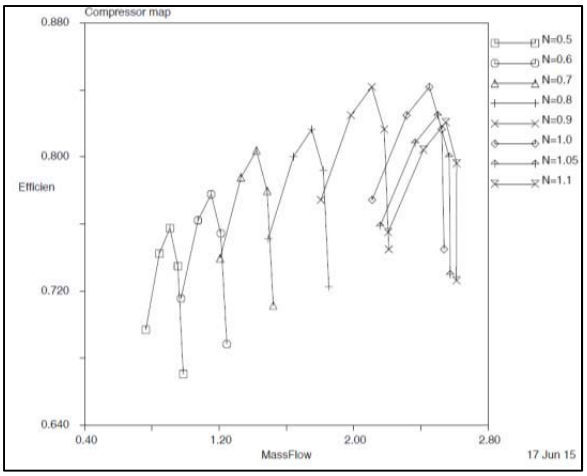

Figure 5: Compressor Efficiency Map for Engine C

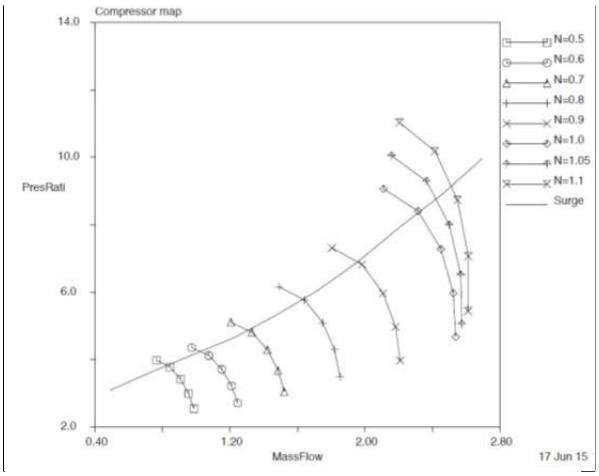

Figure 6: Mass Flow v. Pressure Ratio Map for Engine C

2. Turboshaft Engine Real Cycle

This section presents the real cycle for the three representative turboshaft engines. The following parameters are used in the real cycle calculation:

H – real static state at turboshaft inlet
H* – stagnation state at turboshaft inlet
1* – stagnation state at compressor inlet
2i* – ideal stagnation state at compressor exit
2* – stagnation state at compressor exit
3* – stagnation state at the exit from the combustor
4i* – ideal stagnation state at the exit from the gas generator turbine
4* – stagnation state at the exit from the gas generator turbine
45i* – ideal stagnation state at the exit from the power turbine
45* – stagnation state at the exit from the power turbine
5i – ideal static state at the exit nozzle
5 – real static state at the exit nozzle

2.1 Turboshaft Engine A

Table 7
Real Cycle for Turboshaft Engine A

State	Enthalpy, h [kJ-kg^{-1}]	Temperature, T [°K]	Entropy, s [kJ-(kg-°K)$^{-1}$]	Pressure, p [bar]
H	288.3	288.2	6.6608	1.0000
H*	288.3	288.2	6.6608	1.0000
1*	288.3	288.2	6.6666	0.9800
2i*	505.1	502.1	6.6666	6.9580
2*	551.1	546.5	6.7545	6.9580
3*	1616.6	1436.5	7.9997	6.7493
4i*	1314.4	1194.8	7.9997	3.0288
4*	1347.6	1221.7	8.0274	3.0288
45i*	1152.6	1062.0	8.0274	1.6686
45*	1177.9	1083.0	8.0510	1.6686
5i	1036.5	964.9	8.0510	1.0000
5	1042.1	969.6	8.0658	1.0000

CONTINUED ON NEXT PAGE

2.2 Turboshaft Engine B

Table 8
Real Cycle for Turboshaft Engine B

State	Enthalpy, h [kJ-kg^{-1}]	Temperature, T [°K]	Entropy, s [kJ-(kg-°K)$^{-1}$]	Pressure, p [bar]
H	288.3	288.2	6.6608	1.0000
H*	288.3	288.2	6.6608	1.0000
1*	288.3	288.2	6.6666	0.9800
2i*	543.8	539.5	6.6666	9.0160
2*	588.9	582.8	6.7471	9.0160
3*	1573.8	1410.2	7.8847	8.4750
4i*	1237.8	1137.8	7.8847	3.3862
4*	1264.7	1159.9	7.9077	3.3862
45i*	1089.6	1014.3	7.9077	1.9276
45*	1108.9	1030.5	7.9265	1.9276
5	938.2	885.2	7.9283	1.0302

2.3 Turboshaft Engine C

Table 9
Real Cycle for Turboshaft Engine C

State	Enthalpy, h [kJ-kg^{-1}]	Temperature, T [°K]	Entropy, s [kJ-(kg-°K)$^{-1}$]	Pressure, p [bar]
H	288.3	288.2	6.6608	1.0000
H*	288.3	288.2	6.6608	1.0000
1*	288.3	288.2	6.6608	1.0000
2i*	522.6	519.0	6.6608	8.0000
2*	581.2	575.4	6.7681	8.0000
3*	1565.5	1400.0	7.9148	7.7200
4i*	1210.0	1112.3	7.9148	2.8724
4*	1232.4	1130.8	7.9356	2.8724
45i*	974.9	914.9	7.9356	1.1896
45*	1005.8	941.2	7.9688	1.1896
5i	989.1	927.0	7.9688	1.0860
5	990.4	928.1	7.9785	1.0860

3. Effects of Methane Ingestion on the Turboshaft Real Cycle

This section presents the effect of methane ingestion on the turboshaft real cycle. The first part explores the possibility of methane ignition in the compressor. The second part explores the result of methane ignition in the combustor.

3.1 Effects of Methane Ingestion on the Compressor

Methane ingestion changed the properties of the working fluid in the compressor. Therefore, the real cycle states that define the processes up to the combustor were recalculated for various fractions of methane ingestion compared to the real cycle values presented in Section 2 above.

3.1.1 Turboshaft Engine A

Table 10 presents the real cycle states between the inlet and the combustor, without and with methane ingestion. All concentrations are reported by mass.

Table 10
Real Cycle for Turboshaft Engine A
Without and With Methane Ingestion by Mass

State	Enthalpy, h [kJ-kg^{-1}]	Temperature, T [°K]	Entropy, s [kJ-(kg-°K)$^{-1}$]	Pressure, p [bar]
Without Methane Ingestion				
H	288.3	288.2	6.6608	1.0000
H*	288.3	288.2	6.6608	1.0000
1*	288.3	288.2	6.6666	0.9800
2i*	505.1	502.1	6.6666	6.9580
2*	551.1	546.5	6.7545	6.9580
With 5% Methane Ingestion				
H	304.2	288.2	6.9047	1.0000
H*	304.2	288.2	6.9047	1.0000
1*	304.2	288.2	6.9107	0.9800
2i*	528.1	494.1	6.9107	6.9580
2*	575.7	536.2	7.0031	6.9580
With 10% Methane Ingestion				
H	320.0	288.2	7.1486	1.0000
H*	320.0	288.2	7.1486	1.0000
1*	320.0	288.2	7.1549	0.9800
2i*	551.3	487.4	7.1549	6.9580
2*	600.4	527.6	7.2517	6.9580
With 15% Methane Ingestion				
H	335.8	288.2	7.3925	1.0000
H*	335.8	288.2	7.3925	1.0000
1*	335.8	288.2	7.3990	0.9800
2i*	574.5	481.7	7.3990	6.9580
2*	625.1	520.3	7.5002	6.9580

3.1.2 *Turboshaft Engine B*

Table 11 presents the real cycle states between the inlet and the combustor, without and with methane ingestion. All concentrations are reported by mass.

Table 11
Real Cycle for Turboshaft Engine B
Without and With Methane Ingestion by Mass

State	Enthalpy, h [kJ-kg^{-1}]	Temperature, T [°K]	Entropy, s [kJ-(kg-°K)$^{-1}$]	Pressure, p [bar]
Without Methane Ingestion				
H	288.3	288.2	6.6608	1.0000
H*	288.3	288.2	6.6608	1.0000
1*	288.3	288.2	6.6666	0.9800
2i*	543.8	539.5	6.6666	9.0160
2*	588.9	582.8	6.7471	9.0160
With 5% Methane Ingestion				
H	304.2	288.2	6.9047	1.0000
H*	304.2	288.2	6.9047	1.0000
1*	304.2	288.2	6.9107	0.9800
2i*	567.7	529.2	6.9107	9.0160
2*	614.2	569.9	6.9956	9.0160
With 10% Methane Ingestion				
H	320.0	288.2	7.1486	1.0000
H*	320.0	288.2	7.1486	1.0000
1*	320.0	288.2	7.1549	0.9800
2i*	591.7	520.6	7.1549	9.0160
2*	639.7	559.4	7.2439	9.0160
With 15% Methane Ingestion				
H	335.8	288.2	7.3925	1.0000
H*	335.8	288.2	7.3925	1.0000
1*	335.8	288.2	7.3990	0.9800
2i*	615.9	513.4	7.3990	9.0160
2*	665.3	550.5	7.4921	9.0160

3.1.2 *Turboshaft Engine C*

Table 12 presents the real cycle states between the inlet and the combustor, without and with methane ingestion. All concentrations are reported by mass.

Table 12
Real Cycle for Turboshaft Engine C
Without and With Methane Ingestion by Mass

State	Enthalpy, h [kJ-kg^{-1}]	Temperature, T [°K]	Entropy, s [kJ-(kg-°K)$^{-1}$]	Pressure, p [bar]
Without Methane Ingestion				
H	288.3	288.2	6.6608	1.0000
H*	288.3	288.2	6.6608	1.0000
1*	288.3	288.2	6.6666	0.9800
2i*	522.6	519.0	6.6666	7.8400
2*	572.3	566.9	6.7584	7.8400
With 5% Methane Ingestion				
H	304.2	288.2	6.9047	1.0000
H*	304.2	288.2	6.9047	1.0000
1*	304.2	288.2	6.9107	0.9800
2i*	546.0	510.0	6.9047	8.0000
2*	606.4	563.2	7.0176	8.0000
With 10% Methane Ingestion				
H	320.0	288.2	7.1486	1.0000
H*	320.0	288.2	7.1486	1.0000
1*	320.0	288.2	7.1549	0.9800
2i*	569.5	502.5	7.1486	8.0000
2*	631.9	553.1	7.2670	8.0000
With 15% Methane Ingestion				
H	335.8	288.2	7.3925	1.0000
H*	335.8	288.2	7.3925	1.0000
1*	335.8	288.2	7.3990	0.9800
2i*	593.2	496.1	7.3925	8.0000
2*	657.6	544.7	7.5163	8.0000

3.2 Effects of Methane on the Combustor

This section presents the effect of methane ignition in the combustor on the turbine inlet temperature, (TIT, T_3*). The TIT was calculated from the energy conservation equation discussed in the methodology. It was assumed that the mass flow rate of fuel (Jet A) did not change immediately after methane ingestion, that is, the fuel control unit scheduler did not have sufficient time to adjust to the lower amount of combustion air. Therefore, the temperature reached immediately after methane ingestion is the top limit for the engine, since subsequently the fuel scheduler should reduce the mass flow rate of fuel (Jet A) once the methane ignites in the combustor.

When calculating the TIT variation as a function of the mass flow rate of methane ingested, it was assumed that 90% of the lower heating value of methane, which is 50,050 kJ-kg^{-1}, was transferred to the working fluid. It was also assumed that the lower heating value of Jet A is 43,136 kJ-kg^{-1}, which is identical to the value used for Engine C, but different from the value previously used for Engines A and B (see Figure 7).

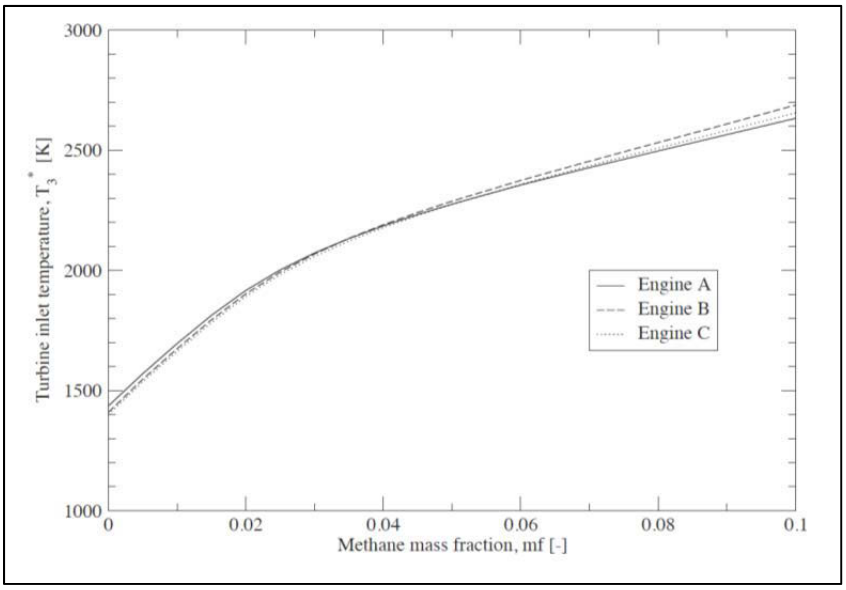

Figure 7: TIT Variation as Function of Mass Fraction of Methane

If the amount of methane in air is given by volume, then the correlation between mass fraction and volume fraction can be obtained from Figure 8. The methane volume fraction range (1% to 18%) corresponds to a mass fraction range of 0.55% to 10.83%.

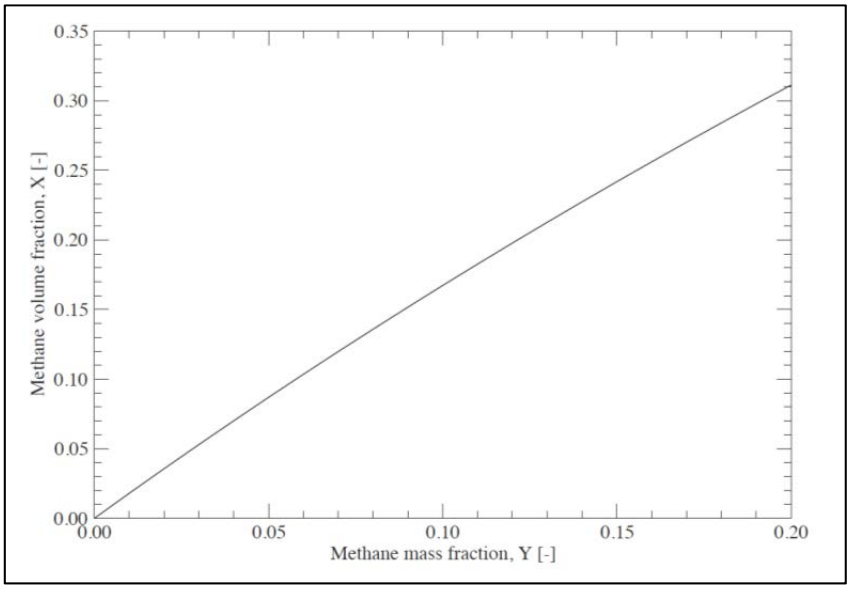

Figure 8: Conversion of Methane Mass Fraction to Volume Percent

DISCUSSION AND CONCLUSIONS

Effect of Methane Ingestion on the Compressor

Data calculated by the mathematical modelling show that methane ingestion slightly reduces temperature at the exit of the compressor. In all representative turboshaft engines, the temperature at the exit of the compressor is below the minimum autoignition temperature of 810°K (Robinson and Smith, 1986). Even if the temperature would exceed the minimum auto-ignition temperature, the flow strain would require an even higher temperature for auto-ignition. Therefore, it is unlikely within a reasonable degree of engineering and scientific certainty that the methane will ignite in the compressor due to adiabatic heating.

Effect of Methane on the Combustor and Concurrent Effects on Compressor and Power Output

The methane will certainly ignite in the combustor. Consequently, the turbine inlet temperature (TIT) will sharply increase. For a methane volume fraction ranging between 1% and 18%, the temperature will increase between approximately 120 °K to 1,100 °K. Depending on the temperature rise, the pressure of in the combustor section will rise with two effects. First, the back pressure on the compressor will rapidly increase, upsetting the operating point and moving it beyond the surge line on the compressor map, more likely than not resulting in a compressor stall and surge. Second, the increase in combustor pressure will increase the N1 and N2 turbine speeds not commanded by the fuel control system. The fuel control system will sense this as an overspeed condition and decrease the fuel schedule, even to the flight idle underspeed governor limit, causing an uncommanded power rollback as the methane fuel enrichment is rapidly exhausted. Recovery of the engine output power depends on the type of fuel control unit (HMFC, ECU, or FADEC) and the control inputs of the operator. Because the effects of the methane ingestion are so rapid, there is insufficient reaction time for the pilot to diagnose the condition and would have no option but to initiate an autorotation in response to a perceived complete engine failure.

Even small mass fractions of methane, as low as 0.4% by volume, may cause a power loss in the representative engines.

Methane Flammability Limits and Ignition Energy

Although this analysis considered methane within the flammability limits of 4.4 to 15 percent by volume, methane has a very low ignition energy value of 0.29 mJ (IChemE, 2007). Practically speaking, if a helicopter were to enter a methane vapor cloud within the flammability limits, ignition sources from hot engine parts, exhaust gas temperatures, and static electricity generated by the rotors would be sufficient to cause a vapor cloud explosion. Therefore, the effect of methane ingestion on turboshaft engine operating points within the flammability limits may be disregarded.

Turboshaft Fuel Control Systems

Turboshaft engines are typically equipped with one of three types of fuel control systems – hydromechanical fuel control units (HMFC), electronic fuel control trimming (ECU), and full-authority digital electronic control (FADEC) (Otis, 1997).

The hydromechanical fuel control system is a fuel metering device that consists of an engine-drive fuel pump, a fuel control unit (FCU), a fuel metering section, power turbine governor, and a fuel distribution manifold and injection nozzles (Lombardo, 1993). The FCU determines the fuel schedule of the engine to provide the required power output and for controlling the speed of the compressor turbine. Engine power output is directly dependent upon compressor turbine speed. Control of the compressor turbine is accomplished by regulating the amount of fuel supplied to the combustion section of the engine through the distribution manifold and injection nozzles. The FCU contains a fuel metering section. The FCU is supplied with fuel from the engine-driven fuel pump at pump pressure. Fuel flow to the combustion section is governed by a main metering valve. The pneumatic fuel computing section senses compressor inlet pressure (Pc) through a pneumatic line connected to the compressor discharge scroll. As discussed above, the FCU controls engine power output by controlling the gas producer speed. Gas producer speed levels are established by the action of the power turbine fuel governor which senses power turbine speed (N2). The power turbine (load) speed is selected by the operator through the control of the collective and power required to maintain this speed is automatically maintained by power turbine governor action on metered fuel flow. The power turbine governor lever schedules the power turbine governor requirements. The power turbine governor schedules the gas producer speed to a changed power output to maintain output shaft speed.

An electronic fuel control unit (ECU) is basically a hydromechanical fuel control with an electronic trimming system which gives the engine better acceleration response and enhanced compressor stall protection (Treager, 2001). The system uses a number of electronic sensors for compressor speed (N1), power turbine speed (N2), compressor pressure (Pc), collective control angle, and turbine gas temperature (TGT). The sensors provide analog electric signals, typically 4-20 mA, to the electronic engine control unit (ECU). The ECU then computes the fuel required fuel schedule based on the programed operating parameters and power demand and actuates a proportional fuel control solenoid on the hydromechanical fuel control unit to maintain the desired power output. In the event of a failure of the ECU, the hydromechanical fuel control can act as a backup fuel control and the ECU can be manually overridden by the operator.

Most modern helicopters are equipped with a full-authority digital engine control (FADEC). The FADEC consists of a digital computer, referred to as the electronic engine controller (EEC), engine control unit (ECU), or the electronic engine control unit (EECU), and its related accessories that control all aspects of aircraft engine performance. A true FADEC has no form of manual override available, placing full authority over the operating parameters of the engine in the decision algorithms of the EECU.

The EECU is a programmable logic controller (PLC) which has proportional-integral-derivative (PID) control. The PID controller calculates an error value as the difference between measured engine parameters and their desired operating points. The PID controller minimizes the error by adjusting the engine power through use of a manipulated variable in fuel scheduling. For optimum control of the engine, the PID is overlaid with a digital Kalman filter. The Kalman filter uses a linear quadratic estimation algorithm that uses a series of engine parameter measurements observed over time which contain statistical noise and other inaccuracies and produces estimates of unknown variables that tend to be more precise than those based on the engine parameter measurements alone. The PID-Kalman filter optimum FADEC provides robust control of engine operation and protects against starting anomalies, compressor stall and surge, and over-torque, over-temperature, or flameout conditions without operator monitoring or intervention.

The FADEC controls the power output of the engine by controlling power turbine independently of the power demand of the engine by very fine adjustments of the gas producer. The EECU provides fuel flow modulation through output signals to a stepper motor driving a fuel metering valve on the hydromechanical fuel control unit. The EECU receives multiple input variables of the current flight condition including air density, collective control position, compressor and turbine temperatures and pressures, and bleed valve position over a digital data bus. These parameters are analyzed multiple times per second and corrections to the gas generator through fuel scheduling are applied, giving precise, fault-tolerant optimum control over engine power output for any given flight condition.

Fuel Control Response to Methane Ingestion

Hydromechanical fuel control units, while robust and not as complex as electronic control units, are probably not as resistant to transient conditions such as a compressor stall or TIT spikes caused by a methane ingestion event. Electronic fuel trimming systems, while more efficient than HMFC, are more likely than not any more resistant to the type of transient conditions caused by methane ingestion. FADEC systems that incorporate a signal to noise control filtering system such as a Kalman filter, however, are more likely than not to be resistant to engine power perturbations caused by small methane ingestion events (<0.4%). However, the actual performance of the fuel control units cannot be modeled or determined without empirical testing on a turboshaft engine so equipped.

REFERENCES

Lombardo, D. (1993). Advanced aircraft systems. New York: McGraw-Hill, Inc.

Institution of Chemical Engineers (IChemE) (2007). LNG fire protection and emergency response. London: Author.

Otis, C. E. (1997). Aircraft gas turbine powerplants. Englewood, CO: Jeppesen Sanderson, Inc.

Robinson, C. and D. B. Smith (1986). The auto-ignition temperature of methane. *Journal of Hazardous Materials 8*, 199–203.

Treager, I. E. (2001). Aircraft gas turbine engine technology, 3d Ed. Columbus, OH: Glencoe/McGraw-Hill, Inc.